FERMILAB-TM-2428-AD

Collective Instability Issues of the Proton Beam for the Muon-to-Electron Conversion Experiment

K. Y. Ng

Fermilab, P.O. Box 500, Batavia, IL 60510

(April, 2009)

Abstract

Stability issues of the proton beam for the muon-to-electron conversion experiment are discussed. These include space-charge distortion of bunch shape, microwave instabilities, mode-coupling instabilities, head-tail instabilities, as well as electron-cloud effects.

1 Introduction

The proton beam destined to hit a target to produce pions which decay into muons for the muon-to-electron conversion experiment has to meet some very stringent specifications. The proton bunchess are first produced in the Fermilab Booster, then coalesced in the Recycler Ring into four bunches, which are then stored in the Accumulator, and next injected one at a time into the Debuncher. The protons are finally extracted in slow spills to the pion-production target. The beam-preparation scenario has been improved by Syphers [1]. The most significant difference will be that the new scheme would send bursts of protons from the Debuncher with an increased intensity. Rather than 12 Tp spilled over 600 ms in the old proposal [2], there would be 1 Tp spilled over about 16 ms. That is, rather than 3.4×10^7 per burst, there would be $\sim 10 \times 10^7$ per burst. The macro-duty factor would be on the order of 30% (6 Booster cycles out of 20 during a Main Injector ramp). The total beam intensity in the Accumulator is cut by a factor of three (12 Tp to 4 Tp), and in the Debuncher by a factor of 12 (from 12 Tp to 1 Tp). The space-charge tune shift in the Debuncher is reduced by the same factor to a congenial $\Delta\nu \sim 0.008$. The momentum spread generated in the Recycler and maintained in the Accumulator and Debuncher would be a factor of four less (0.2% rather than 0.8%).

The purpose of this article is to study the beam inside the various rings in the collective-instability aspects. We will study the influence of space charge on bunch distortion in the longitudinal phase space and then the possibility of microwave instability. The accumulation of electron cloud by the intense proton bunches are next addressed, followed by the possibility of two-stream coupled oscillation instability. We next study limit of the transverse mode-coupling instabilities, and finally head-tail growth rates. A conclusion is given at the end.

2 Space Charge and Bunch Lengthening

When each intense bunch is formed by coalescing 21 Booster bunches in the Recycler, strong space charge can distort the bunch shape, leading to bunch lengthening. Equations of motion of a particle in an rf potential consisting of a number of rf systems with harmonics h_i and

voltages V_i are

$$\begin{aligned}\frac{d\tau}{dt} &= -\frac{\eta}{\beta^2 E}\Delta E,\\ \frac{d\Delta E}{dt} &= \frac{1}{T_0}\sum_i eV_i \sin(\phi_s - h_i\omega_0\tau),\end{aligned} \tag{2.1}$$

where ΔE is the energy offset and τ is the time advance with respect to the synchronous particle. In above, η is the slip parameter, $T_0 = 2\pi/\omega_0$ is the revolution period, $v = \beta c$ is the beam nominal velocity, and ϕ_s is the synchronous phase.

Longitudinal space-charge force kicks the beam imparting energy to tbe beam particle at the rate of $d\Delta E/dt = eE_s v$, where E_s is the longitudinal space-charge electrical field at the bunch and is given by

$$E_s = -\frac{eN_b g_0}{4\pi\epsilon_0\gamma^2}\frac{d\rho}{d\tau}, \tag{2.2}$$

with N_b being the number of particles in the bunch having the longitudinal or linear distribution $\rho(\tau)$ normalized to unity when integrated over τ. The second equation of motion therefore becomes

$$\frac{d\Delta E}{dt} = -\sum_i \frac{eV_i}{T_0}\sin(\phi_s - h_i\omega_0\tau) - \frac{e^2 N_b}{2\pi}\left|\frac{Z_\parallel}{n}\right|\frac{d\rho}{d\tau}, \tag{2.3}$$

where $Z_\parallel/n = iZ_0 g_0/(2\beta\gamma^2)$ is the longitudinal space-charge impedance and $g_0 = 1 + 2\ln b/a$ is the space-charge parameter with b and a being the vacuum chamber and beam radii, and $Z_0 = 376.7\ \Omega$ is the free-space impedance.

To obtain the trajectory of a particle, we eliminate the time t from the equations of motion by dividing one equation of motion by the other to arrive at the differential equation,

$$\Delta E\frac{d\Delta E}{d\tau} = \frac{\beta^2 E}{\eta}\left[-\sum_i \frac{eV_i}{T_0}\sin(\phi_s - h_i\omega_0\tau) - \frac{e^2 N_b}{2\pi}\left|\frac{Z_\parallel}{n}\right|\frac{d\rho}{d\tau}\right]. \tag{2.4}$$

The trajectory that goes through $\Delta E = 0$ and $\tau = \sigma_\tau$, the rms bunch length, is represented by

$$(\Delta E)^2 = \frac{2\beta^2 E}{\eta}\left\{\sum_i \frac{eV_i}{2\pi h_i}\big[\cos(\phi_s - h_i\omega_0\tau) - \cos(\phi_s - h_i\omega_0\sigma_\tau)\big] - \frac{e^2 N_b}{2\pi}\left|\frac{Z_\parallel}{n}\right|\big[\rho(\tau) - \rho(\sigma_\tau)\big]\right\}. \tag{2.5}$$

The area covered by this trajectory is the rms bunch area σ_A, and is given by

$$\sigma_A = \int_0^{\sigma_\tau} d\tau \left\{ \frac{32\beta^2 E}{\eta} \left[\sum_i \frac{eV_i}{2\pi h_i} \big[\cos(\phi_s - h_i\omega_0\tau) - \cos(\phi_s - h_i\omega_0\sigma_\tau) \big] - \frac{e^2 N_b}{2\pi} \left| \frac{Z_\parallel}{n} \right| \big[\rho(\tau) - \rho(\sigma_\tau) \big] \right] \right\}^{\frac{1}{2}}. \tag{2.6}$$

Here the only unknown is the linear distribution function $\rho(\tau)$, which can be approximated by a Gaussian. We see that the space-charge force counteracts the rf force below transition ($\eta < 0$, $0 < \phi_s < \frac{1}{2}\pi$), and enhances the rf force above transition ($\eta > 0$, $\frac{1}{2}\pi < \phi < \pi$). For example, if the space-charge force is large enough below transition, the expression inside the curly brackets of Eq. (2.5) will change sign making $(\Delta E)^2 < 0$. The implication is the space-charge repulsive force is larger than the rf focusing force, so that rf bunching becomes unavailable.

To coalesce 84 bunches into 4, it is best to start with the completely linear barrier voltage first [3]. After a while the $h = 28$ $V = 80$ kV rf, which is much stronger than the barrier voltage of 2 kV, is employed. If one uses the $h = 28$ rf directly (without using first the barrier voltage), the bucket of the rf is not large enough to enclose the bunches at the edge, leading to particle loss. A more linear rf is favored in rf rotation. This can be performed by adding a little amount of 2nd or 3rd harmonic. Since the second harmonic goes to zero when the first harmonic reaches a maximum, in order to make the region between $\pm\pi/2$ (for first harmonic) more linear, the second harmonic must therefore be out-of-phase. Thus this second harmonic will counteract part of the first harmonic. The bunch length will therefore increase as soon as the second harmonic is turned on.

Below transition, space-charge is repulsive and will lengthen the bunch. As a measure of the effect, we introduce the parameter $f_{\rm spch}$, which is defined as the ratio of the linear space-charge force to the linear rf force. Through Eq. (2.3),

$$f_{\rm spch} = \frac{\text{linear spch}}{\text{linear rf}} = \frac{\frac{e^2 N_b |Z_\parallel/n|}{2\pi} \frac{1}{\tau} \frac{d\rho}{d\tau}}{\sum_i \frac{eV_i}{T_0} h_i \omega_0}. \tag{2.7}$$

For Gaussian distribution near $\tau = 0$,

$$f_{\rm spch} = \frac{eN_b |Z_\parallel/n|}{\sqrt{2\pi} \sum_i V_i h_i \omega_0^2 \sigma_\tau^3}. \tag{2.8}$$

The rms normalized vertical emittance of a Booster bunch near extraction has been measured by Huang [4] to be $\epsilon^n_{\rm rms} = 6.5$ πmm-mr. We assume perfect matching in the

Table I: Some properties of the Recycler, Accumulator, and Debuncher.

	Recycler	Accumulator	Debuncher
Circumference (m)	3319.418	474.098	505.283
Transition gamma	19.968	6.549	7.640
Rf V_1/h_1 (kV)	80/28	100/4	30/4
V_2/h_2 (kV)	−16/56		

transfer of the beam to the Recycler. The mean vertical betatron function of the Recycler is $\bar{\beta}_y = R/\nu_y = 528.3/24.4 = 21.6$ m. Thus the rms vertical beam radius in the Recycler will be $\sigma_y = \sqrt{\epsilon_n \bar{\beta}_y/(\gamma\beta)} = 3.85$ mm. The vacuum chamber of the Recycler is elliptical with horizontal and vertical radii $(a, b) = (0.0476, 0.0222)$ m. The space-charge coefficient is $g_0 = \gamma_e + 2\ln(b/\sqrt{2}\sigma_y) = 3.3704$, γ_e being the Euler number. Then $Z_\parallel/n = i7.03\ \Omega$. The Recycler has a revolution frequency of $\omega_0/2\pi = 89.82$ kHz. Some properties of the Recycler, Accumulator, and Debuncher are listed in Table I. The full bunch area in Booster is 0.1 eVs. Injected into the Recycler, a Booster batch forms 4 bunches, each consists of 21 former booster bunches. If the coalescence is perfect without phase space dilution, each of these 4 bunches will have an rms area of $21 \times 0.1/6 = 3.5$ eV-s. The matched rms length is $\sigma_\tau = 17.7$ ns after solving Eq. (2.6). We obtain $f_{\rm spch} = 0.0783$, which is not too small. However, the present coalescence scheme does enlarge the bunch area. If the enlargement is 3-fold, the rms bunch length becomes $\sigma_\tau = 31.5$ ns while the space charge parameter decreases to $f_{\rm spch} = 0.021$, which is pretty small.

3 Microwave Instabilities

After 4 bunches are formed in the Recycler, $\sigma_\tau = 31.5$ ns, $\sigma_E = 10.63$ MeV. With $N_b = 1 \times 10^{12}$ particles in each bunch, the peak current is $I_{\rm pk} = eN_b/(\sqrt{2\pi}\sigma_\tau) = 2.028$ Amp. The longitudinal microwave Keil-Schnell stability limit is

$$\left|\frac{Z_\parallel}{n}\right| < \frac{2\pi|\eta|E}{eI_{\rm pk}}\left(\frac{\sigma_E}{E}\right)^2 = 333\ \Omega, \tag{3.1}$$

which is very large. The longitudinal impedance per harmonic of the Recycler has been studied [5]. The impedance consists of $Z_{\rm gap} = 209\ \Omega$ at 50 kHz for the cavities, $Z_{\rm rm} = 26\ \Omega$ peaking at ~ 3 kHz for the resistive-wall monitor, and $Z_{\rm wall} = (1-i)7.58\ \Omega$ at the revolution frequency for the resistivity of the stainless steel beam pipes. The BPM's contribution is

Table II: Matched longitudinal bunch sizes and microwave stability limits of the $N_b = 1 \times 10^{12}$ bunch inside the Recycler, Accumulator, and Debuncher. The space-charge impedance is assumed to be $i7.03\ \Omega$ for the bunch in all three rings.

	σ_τ (ns)	σ_E (MeV)	$I_{\rm pk}$ (A)	$\lvert Z_\parallel/n\rvert$ limit (Ohms)
rms bunch area = 1.05 *eVs, blown-up 3 times*				
Recycler	31.52	10.63	2.028	333.1
Accumulator	19.90	16.81	3.212	760.8
Debuncher	23.27	14.39	2.747	323.8
rms bunch area = 1.40 *eVs, blown-up 4 times*				
Recycler	36.43	12.27	1.755	513.6
Accumulator	23.01	19.39	2.777	1170.
Debuncher	26.94	16.58	2.373	494.7
rms bunch area = 1.575 *eVs, blown-up 4.5 times*				
Recycler	38.67	13.01	1.653	613.0
Accumulator	24.43	20.56	2.617	1229.
Debuncher	28.60	17.57	2.235	497.7
rms bunch area = 1.75 *eVs, blown-up 5 times*				
Recycler	40.00	13.45	1.578	677.8
Accumulator	25.76	21.66	2.481	1635.
Debuncher	30.17	18.51	2.119	694.7

much smaller. Since these are much less than the Keil-Schnell limit, there will not be any microwave instability.

These bunches are next injected into the Accumulator and finally the Debuncher. The slip factors in the Accumulator and Debuncher are, respectively, $\eta = +0.01229$ and $+0.006113$. We computed the rms bunch length and rms energy spread, and finally the limited $Z_\parallel/n$ microwave stability limit. The results are listed in Table II. The coupling impedance of the Accumulator had been studied in detail before the ring was built [6]. The longitudinal impedance per harmonic is small; for example the broad resonance in the connecting bellows contributes only $Z_\parallel/n = 0.3\ \Omega$. So there will not be any possibility of meeting with microwave instabilities.

The coupling impedance of the Debuncher has never been tabulated. The beam pipes

and their transitions, however, have been tabulated in detail in a spreadsheet. It turns out that the beam pipes have rather large apertures, since it is the first stage of the antiproton cooling system. Its purpose is to accept pulses of antiprotons from the AP-2 line and to reduce their momentum and transverse phase space for efficient transfer to the Accumulator. The average radius of the vacuum chamber is 10 cm. As a result, the resistive wall impedance will be small. In short, the coalesced bunches should be safe against microwave instabilities.

4 Electron Cloud

4.1 Cloud Simulations

Proton bunches of high intensity will attract electron clouds. We will first study the situation of the Accumulator, where the four bunches, each of intensity $N_b = 1 \times 10^{12}$ and rms length $\sigma_\tau = 40$ ns, are equally spaced. The code POSINST [7] has been employed to simulate the production of electrons. The stainless steel beam pipe have an elliptical cross-section of horizontal and vertical radii $a = 7$ cm and $b = 5$ cm. The transverse rms bunch radii are $\sigma_x/\sigma_y = 2.74/2.41$ mm. A peak secondary electron yield (SEY) of 2.0 is assumed. The electron-cloud density averaged over one sigma of the beam ellipse is shown in Fig. 1 as a function of rf bucket number (or bunch number here). Superimposed is the electron-cloud density averaged over the whole vacuum chamber. We see that it requires about the distance of 6 rf buckets or one and a half revolution turns for the electron cloud to build up to the average density of $\rho_e \sim 2 \times 10^{12}$ m^{-3} when averaged over the one sigma ellipse of the bunch.

As for the Debuncher, the beam pipe is of larger aperture, roughly 10 cm radius. However, there will only be a single bunch and the 3 consecutive empty rf bucket serves as a very wide gap. A similar POSINST simulation shows in Fig. 2 that the electron density, built up in the presence of the bunch, falls back to zero in the gap. The electron density within one sigma of the beam averaged to only $\rho_e \sim 4 \times 10^{10}$ m^{-3}.

The Recycler is close to 7 times as large as the Accumulator and Debuncher. The 4 coalesced proton bunches occupy 4 consecutive rf buckets in the $h = 28$ rf system. Thus there are 24 empty rf buckets for the electrons to subside before encountering the 4 proton bunches again in the next revolution turn. According to simulation of the Accumulator, electron cloud density can build up to about $\rho_e \sim 3 \times 10^{11}$ m^{-3} only with 4 bunches in a row

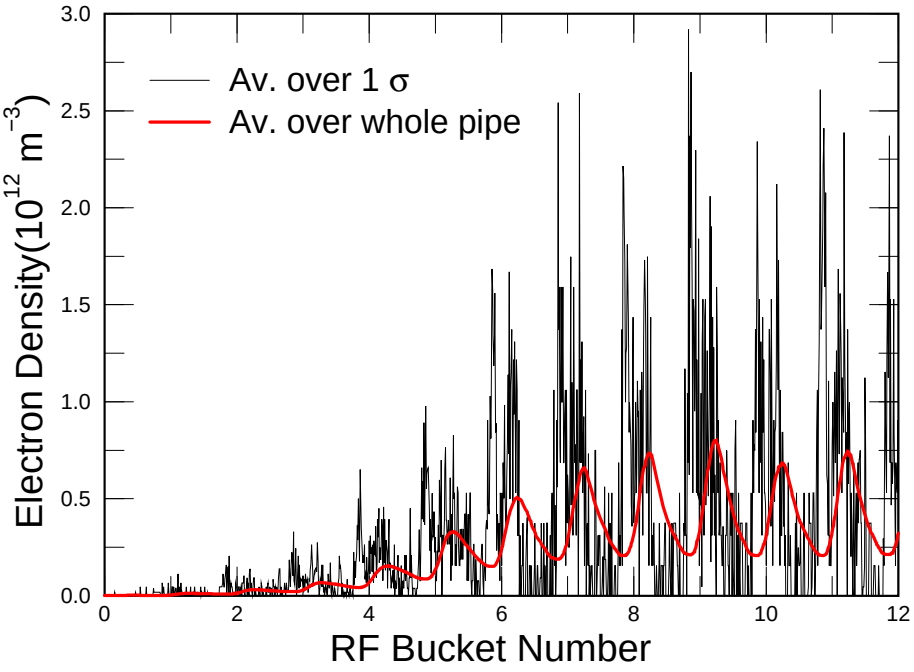

Figure 1: (Color) Electron cloud density generation in the Accumulator Ring as a function of rf bucket number. One revolution turn is 4 rf buckets. Black: averaged over electrons within one sigma ellipse of the bunch. Red: averaged over the whole beam pipe. SEY= 2.0 has been assumed.

when averaged over one sigma. We expect this to be the amount of electron density at the last proton bunch in the Recycler.

4.2 Two-Stream Oscillations

The electron cloud and the proton beam attract each other and can develop coupled two-stream oscillation. Landau damping of the effect comes from the betatron tune spread $\Delta\nu_y$ and the spread of the electron-bounce frequency $\Delta\omega_e$. The stability limit has been derived by Schnell and Zotter [8], which is

$$\frac{\Delta\nu_y}{\nu_y}\frac{\Delta\omega_e}{\omega_p} \gtrsim \frac{9\pi^2}{64}\frac{w_p^2}{\nu_y^2\omega_0^2}, \tag{4.1}$$

where the electron-bounce frequency in the beam potential is

$$\frac{\omega_e}{2\pi} = \frac{c}{2\pi}\sqrt{\frac{2N_b r_e}{\sigma_y(\sigma_x+\sigma_y)\sqrt{2\pi}\sigma_z}}, \tag{4.2}$$

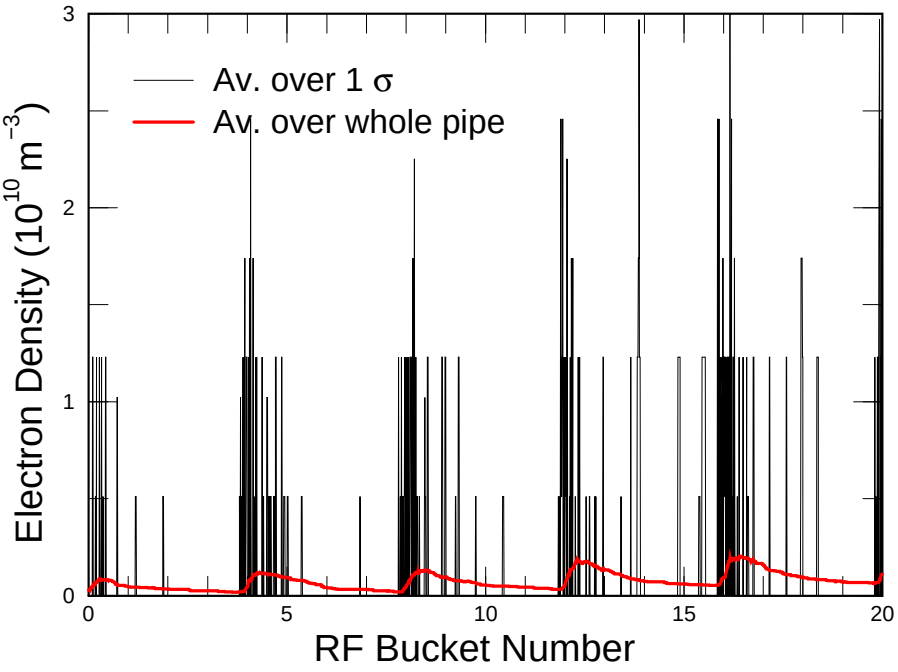

Figure 2: (Color) Electron cloud density generation in the Debuncher Ring as a function of rf bucket number. One revolution turn is 4 rf buckets. Black: averaged over electron within one sigma ellipse of the bunch. Red: averaged over the whole beam pipe. SEY= 2.0 has been assumed.

with $\sigma_z = \sigma_\tau \beta c$, and the proton-bounce frequency in the electron cloud potential in the absence of betatron focusing is

$$\frac{\omega_p}{2\pi} = \frac{c}{2\pi}\sqrt{\frac{\pi \rho_e r_p}{\gamma}}. \tag{4.3}$$

In above, r_e and r_p are the electron and proton classical radii, $\sigma_x = 2.74$ mm and $\sigma_y = 2.41$ mm are the beam radii, $\rho_e = 2 \times 10^{12}$ is the electron-cloud density obtained in the earlier simulation. We obtain $\omega_e/2\pi = 186$ MHz and $\omega_p/2\pi = 48.0$ kHz. The two-stream stability limit becomes

$$\Delta\nu_y \frac{\Delta\omega_e}{\omega_e} \gtrsim 0.0009. \tag{4.4}$$

The spread of electron bounce frequency is usually quite large. Even if we take $\Delta\omega_e/\omega_e \sim 0.1$, a tune spread of $\Delta\nu_y \sim 0.01$ will be sufficient to damp the instability. For the Recycler and Debuncher, the electron-cloud density will be one and two orders of magnitudes smaller. As a result, there will not be any chance for two-stream oscillation instabilities to develop.

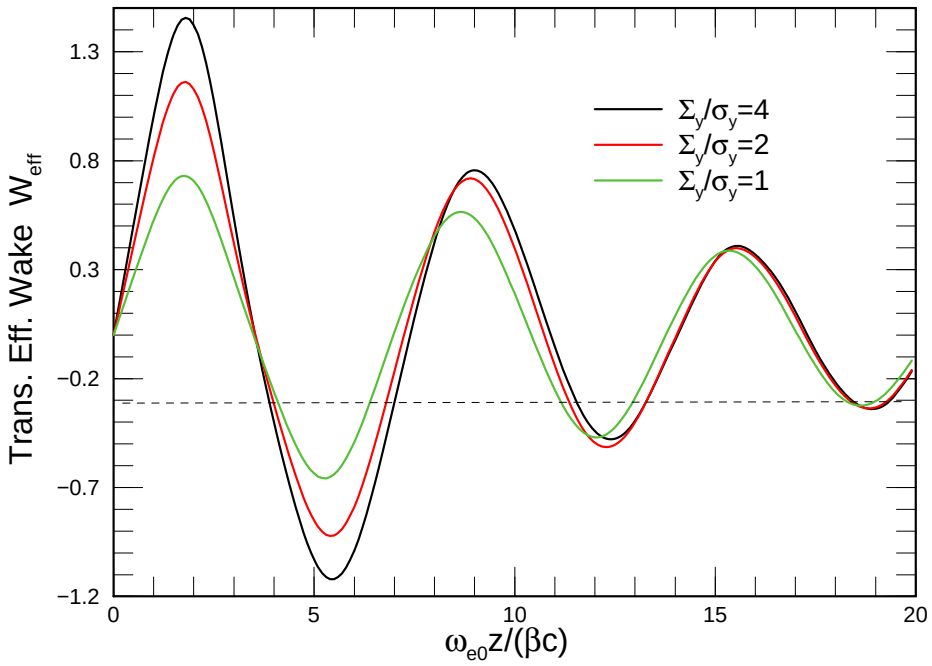

Figure 3: (Color) Effective electron-cloud wake derived by Heifets. A round beam ($p = 1$) is assumed.

4.3 Wake Fields

Electron cloud generate wake fields which will affect the stability of the beam particles. The transverse electron-cloud wake has been derived by Heifets and is given by [9]

$$W_1(z) = \frac{8Z_0\rho_e\omega_e R}{(1+p)\lambda_b^{\rm pk}} W_{\rm eff}(\zeta), \tag{4.5}$$

with the dimensionless length $\zeta = \omega_e z/\beta c$, where $p = \sigma_y/\sigma_x$ is the aspect ratio of the particle beam, with peak linear density $\lambda_b^{\rm pk} = N_b/\sqrt{2\pi}\sigma_z$, R is the radius of the accelerator ring, and $Z_0 \approx 376.7\ \Omega$ is the free-space impedance. The dimensionless effective electron-cloud wake $W_{\rm eff}(\omega_e z/\beta c)$ is shown in Fig. 3 for a round beam ($p = 1$) with transverse rms spread of cloud to rms spread of beam $\Sigma_y/\sigma_y = 1$, 2, and 4. The corresponding transverse impedance is

$$Z_1^{\perp}(\omega) = \frac{8Z_0\rho_e R}{(1+p)\lambda_b^{\rm pk}\beta} Z_{\rm eff}\left(\frac{\omega}{\omega_e}\right), \tag{4.6}$$

where

$$Z_{\rm eff}\left(\frac{\omega}{\omega_e}\right) = i\int_{-\infty}^{\infty} W_{\rm eff}(\zeta) e^{i\omega\zeta/\omega_e} d\zeta. \tag{4.7}$$

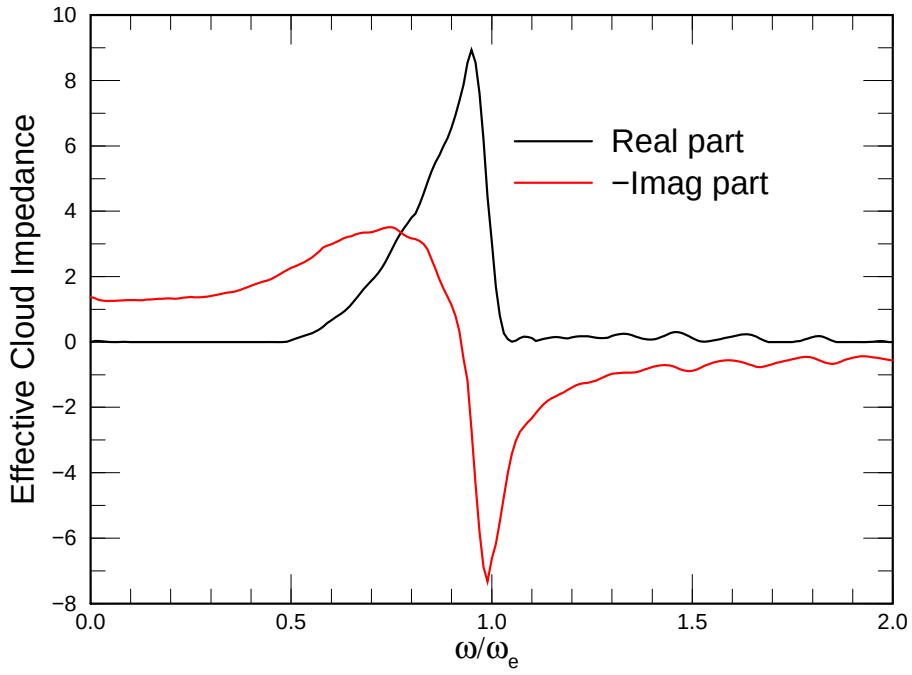

Figure 4: (Color) Real and imaginary parts of the dimensionless reduced electron-cloud impedance for a round beam with $\Sigma_y/\sigma_y = 2$.

Real and imaginary parts of the dimensionless impedance for $\Sigma_y/\sigma_y = 2$ are shown in Fig. 4. A resonance at $\omega = \omega_e$ is evident. Take the Accumulator as an example. For the 1×10^{12}-bunch of rms length $\sigma_\tau = 40$ ns, the accumulated electron-cloud density of $\rho_e = 2 \times 10^{12}$ m^{-3} will lead to a transverse impedance with a resonant peak of ~ 60 MΩ/m at $\omega_e/2\pi = 186$ MHz. This impedance will be employed in the discussion of transverse single bunch instabilities below.

One may be annoyed by the appearance of the linear beam density $\lambda_b^{\rm pk}$ in the denominators of Eqs.(4.5) and (4.6). However, one must understand that the electron density ρ_e that appears in the numerators is a monotonic function of the linear beam density. Although the relationship may not be linear, as $\lambda_b^{\rm pk} \to 0$, we have $\rho_e \to 0$ as well.

5 Transverse Microwave Instability

Similar to the Keil-Schnell limit for longitudinal microwave instability, this is also a coasting-beam limit for transverse microwave instability for coasting beam. The theory is applicable

to bunch beam when the average current replaced by the peak current and when the growth rate is much faster than the synchrotron frequency. The stability limit for the vertical instability is given by

$$Z_1^\perp \lesssim -\frac{4\pi E\beta\nu_y}{ieI_{\rm pk}R}\frac{1}{\sqrt{3}}(\Delta\nu_y)_{\rm HWHM}F. \tag{5.1}$$

For the vertical plane of the Accumulator, $\nu_y = 8.67$. For Gaussian distribution the form factor is $F = \sqrt{3/(\pi\ln 2)} = 1.174$. For a bunch of intensity $N_b = 1\times 10^{12}$ and rms bunch length $\sigma_\tau = 40$ ns, the peak current is $I_p = 1.60$ A. We obtain the limit $|Z_1^\perp| \lesssim 5470(\Delta\nu_y)_{\rm HWHM}$ MΩ/m. Even when the electron-cloud impedance resonant peak of ~ 60 MΩ/m is substituted, a tune spread of $(\Delta\nu_y)_{\rm HWHM} \sim 0.01$ will be sufficient to prevent the instability from occuring.

6 TMCI

Transverse mode-coupling instability (TMCI) occurs for nearly all electron rings. Recently, such instability has also been observed in the CERN SPS [10]. The limit of stability for long bunches driven by a resonance at angular frequency $\omega_r = n_r\omega_0$ can be derived analytically and is given by

$$|Z_1^\perp| \lesssim \frac{16\alpha}{\pi}\frac{|\eta|\omega_r\nu_y A}{\beta^2 ce^2N_b}\left|1+\frac{\omega_\xi}{\omega_r}\right| = \frac{16\alpha}{\pi}\frac{|\eta|n_r\nu_y A}{\beta Re^2N_b}\left|1+\frac{\omega_\xi}{\omega_r}\right|, \tag{6.2}$$

where letting the factor $\alpha = \pi/4$ make the limit exactly the one derived by Métral [11]. With 5-fold increase, the 95% longitudinal bunch area is $A = 10.5$ eVs. The above stability limit becomes $|Z_1^\perp| \lesssim 0.1954n_r$ MΩ/m. This appears to be serious because the rf is chosen to have $h = 4$, whose impedance will drive the instability. The resistive-wall impedance and the electron cloud can also be a driving source. The Accumulator and Debuncher operates above transition with $\eta = 0.01230$ and $\eta = 0.006113$, respectively. However, a small (even negative) chromaticity can increase the stability limit by very much. Since the factor

$$1+\frac{\omega_\xi}{\omega_r} = 1+\frac{\xi}{\eta n_r} \gg 1, \tag{6.3}$$

even with $\xi = 1$, we can rewrite the stability condition as

$$|Z_1^\perp| \lesssim \frac{16\alpha}{\pi}\frac{\xi\nu_y A}{\beta Re^2N_b} = 31.96\xi \text{ MΩ/m}. \tag{6.4}$$

The above limit is derived from the shifting of two neighboring azimuthal modes by the amount of the synchrotron frequency. Unfortunately, this is not the correct way to determine the instability limit, because two modes can cross each other without really coupled together. For a more detailed investigation, we perform a numerical solution of the interaction matrix. The driving force in the computation includes the resistive-wall impedance and the electron-cloud impedance. Let us concentrate on a bunch in the Accumulator, where the electron cloud density is the largest. We set the cloud density as $\rho_e = 2 \times 10^{12}$ m^{-3} at the bunch intensity of $N_b = 1 \times 10^{12}$ and we assume the cloud density varies linearly with the bunch intensity. The chromaticity is set to zero. The interaction matrix is first solved by including azimuthal modes $m = -4,\ -3,\ -2,\ -1,\ 0,\ 1$ and radial modes $k = 0,\ 1,\ 2$. Gaussian modes are assumed. The result is shown in top plot of Fig. 5. We see a lot of numerical noise in the solution, because this is the numerical solution of a matrix of large dimension, 18 by 18. However, it appears that the modes only cross each other without merging. In order to have a clearer understanding, the interaction matrix is next solved with only one radial mode for each azimuthal mode. The solution, shown in the lower plot of Fig. 5 clearly shows that the modes just cross each other without interaction. Comparing the two plots more closely, we can make the conclusion that there is no real mode mixing or instability at least up to the bunch intensity of $N_b = 1.5 \times 10^{12}$.

7 Head-Tail Instabilities

Head-tail instabilities are driven by the transverse wake when the chromaticity $\xi_y \neq 0$. The electron-cloud wake can be important near the electron-bounce frequency $\omega_e/2\pi$. We concentrate on the proton bunch inside the Accumulator, where the electron density $\rho_e \sim 2 \times 10^{12}$ m^{-3} is much higher than those in the other rings. The resistive-wall impedance is also included.

The computed growth or damping rates for azimuthal modes $m = 0,\ \pm 1,\ \pm 2,\ \pm 3$, and ± 4 are shown in Fig. 6. Gaussian modes have been used. The electron-bounce frequency is $\omega_e/2\pi = 186$ MHz. Thus the power spectra of all modes with $|m| \lesssim (\omega_e \sigma_\tau)^2 = 2190$ are in between $\pm\omega_e$ when $\xi_y = 0$. As ξ_y becomes positive, the spectra of these modes will overlap the electron-cloud impedance more at $+\omega_e$ more than at $-\omega_e$, and these modes will be damped. On the other hand, modes with $|m| \gtrsim 2190$ will become unstable. However, the power spectra of such high-azimuthal modes have very tiny amplitudes, and their corresponding

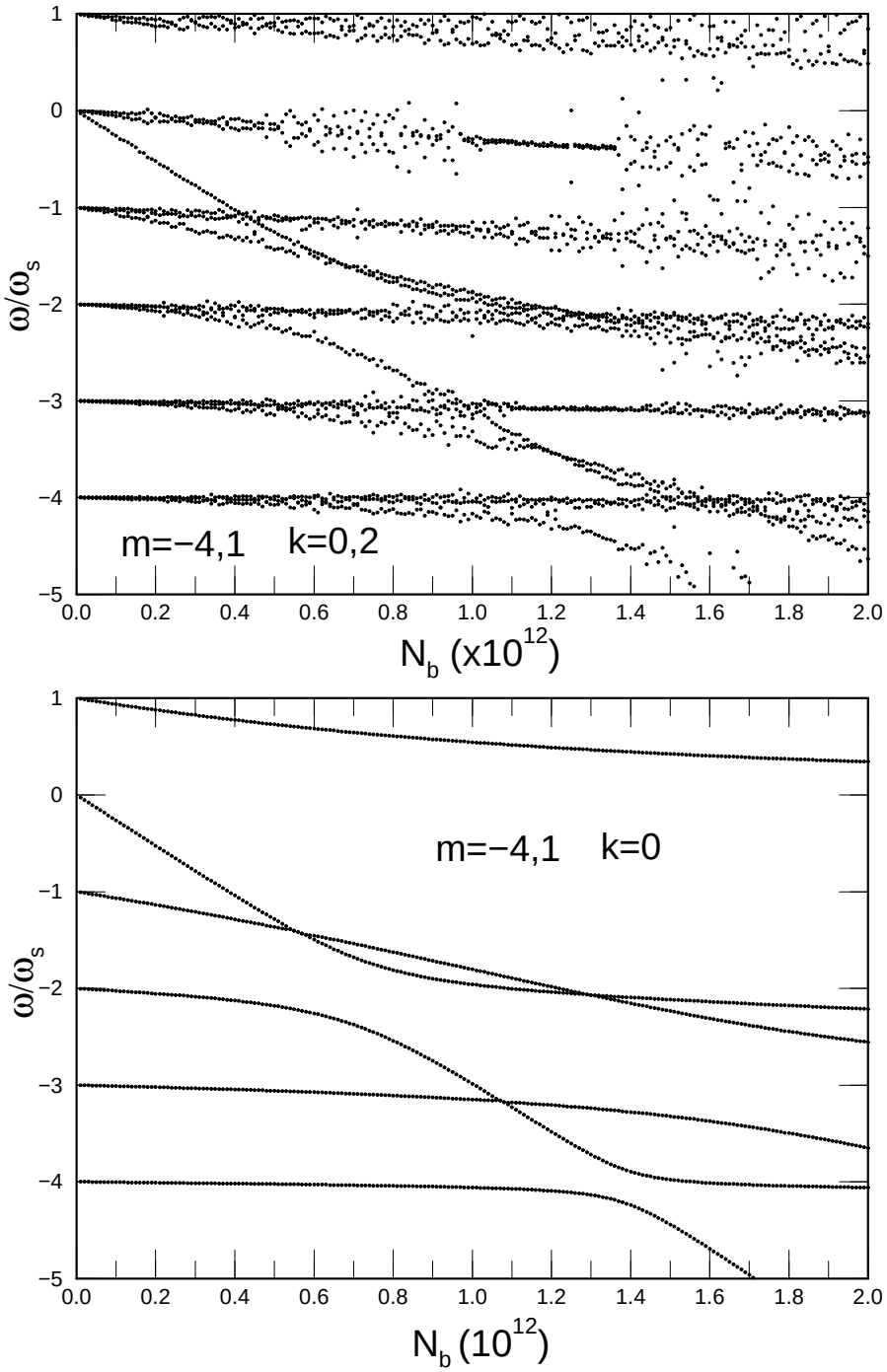

Figure 5: Transverse eigen-states of a bunch in the Accumulator as functions of bunch intensity N_b. Top: Azimuthal modes $m = -4,\ -3,\ -2,\ -1,\ 0,\ 1$ and radial modes $k = 0,\ 1,\ 2$ are included. Bottom: Only one radial mode ($k = 0$) is included for each azimuthal mode. No instability is observed.

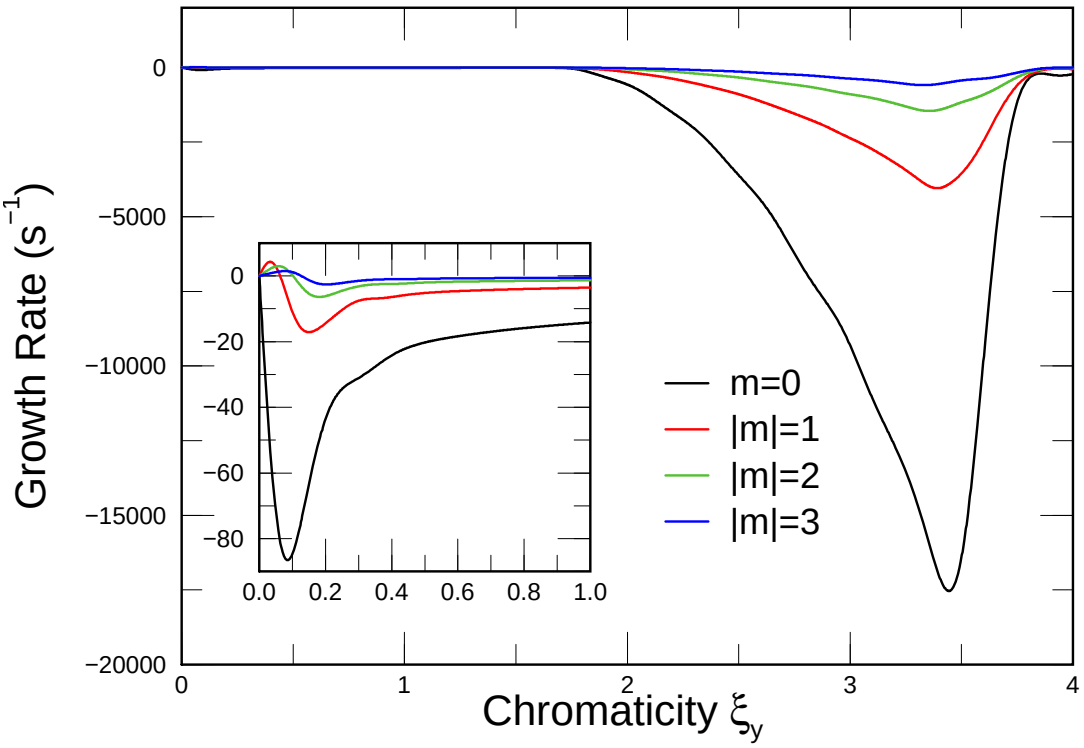

Figure 6: (Color) Head-tail growth rates for azimuthal modes $m = 0, \ , \pm 1, \ \pm 2$, and ± 3 as functions of chromaticity ξ_y. Electron-cloud impedance dominates in the vicinity of $|\xi_y| \sim 3.5$. The insert shows a magnified view for small ξ_y, where the resistive-wall impedance dominates.

growth rates will be very tiny as well, and are therefore unimportant.

The insert in Fig. 6 shows a magnified view for small ξ_y. We see that modes with $|m| > 1$ are unstable. The instabilities are driven by the resistive-wall impedance. Their growth rates are less then ~ 5 s^{-1}, however, and are totally unimportant, because the proton bunches reside in the Accumulator for at most 64 ms only. Nevertheless, these small growths can be ameliorated completely by operating the Accumulator at $\xi_y \gtrsim 0.2$.

As discussed above, the electron-cloud impedance should not drive any head-tail instabilities in the Debuncher and Recycler as well, where the electron-cloud densities will be even smaller. The resistive-wall impedance in the Debuncher will be smaller than that in the Accumulator because of its larger vacuum-chamber aperture. As a result, the above operating criterion for the chromaticity in the Accumulator can be slightly relaxed here. The Recycler, however, is below transition. To avoid head-tail instabilities, we therefore need to operate with slightly negative chromaticity instead.

8 Conclusion

We have studied several beam stability issues of the proton beam heading to the target for the muon-to-electron conversion experiment. The bunch shape distortions driven by the space-charge force is reasonably small, and longitudinal microwave instability will unlikely to occur. Electron-cloud buildup may be appreciable in the Accumulator with electron density up to $\rho_e \sim 2 \times 10^{12}$ m^{-3}. That in the Recycler will be an order of magnitude smaller, and that in the Debuncher will be another order of magnitude smaller. The electron cloud in the Accumulator will not be large enough to drive coupled two-stream oscillation instability. However, it will generate an effective transverse wake field or impedance which can be harmful to single transverse beam stability. Transverse mode-coupling instability appears not to occur in the Accumulator. Various modes of excitation just cross each other without merging. Head-tail instabilities can be severe if the chromaticity shifts the peak of the mode spectra onto the peak of the electron-cloud impedance. However, the effect of the electron-cloud and resistive-wall driving forces can be completely ameliorated by operating the Accumulator at a chromaticity higher than ~ 0.2. The same is true for the Debuncher. As for the Recycler, which is below transition, the operating chromaticity should be chosen slightly negative instead.

References

[1] M. Syphers, *Possible Scheme to Ameliorate Space Charge and Momentum Spread Issues*, mu2e note, 2008

[2] The mu2e Collaboration, *A Letter of Intent: A Muon to Electron Conversion Experiment at Fermilab*, Fermilab TM-2396-AD-E-TD, 2007; C. Ankenbrandt, et al., *Using the Fermilab Proton Source for a μ-e Conversion Experiment*, Fermilab-TM-2368-AD-E, 2006; D. Neuffer, *More Rebunching Options for the μ2e Conversion Experiments*, Fermilab BEAMS-DOC-2787-V1, 2007.

[3] C. Bhat and J. MacLachlan, *RF Requirements for Bunching in the Recycler for Injection into the $g-2$ Ring*, Fermilab Beams-doc-3192, 2008.

[4] Xiaobiao Huang, *Beam Diagnosis and Lattice Modeling of the Fermilab Booster*, PhD thesis, Indiana University, 2005; X. Huang, *The Coherent Detuning of Vertical Beta-*

tron Tunes, 2005, unpublished; X. Huang, *Bunch Length Measurements at Different Intensity*, 2005, unpublished.

[5] K.Y. Ng, *Coherent Parasitic Energy Loss of the Recycler Beam*, Fermilab-TM-2249, 2004.

[6] K.Y. Ng, *Recalculation of Some Impedances of the Accumulator*, Fermilab pbar note 470, 1976.

[7] M.A. Furman and G.R. Lambertson, *The Electron-Cloud Instability in the Arcs of the PEP-II Positron Ring*, LBNL Report LBNL-441123/CBP Notes-246, PEP-II AP Note AP 97.27, Proc. Int. Workshop on Multibunch Instabilities in Future Electron and Positron Accelerators (MBI-97), ed. Y. H. Chin (KEK, Tsukuba, Japan, July 15–18, 1997).

[8] W. Schnell and B. Zotter, CERN Report ISR-GS-RF/76-26, 1976.

[9] S. Heifets, *Wake Field of the e-cloud*, SLAC-PUB-9025, 2001.

[10] H. Burkhardt, G. Arduini, E. Benedetto, E. Métral, and G. Rumolo, *Observation of Fast Single-Bunch Transverse Instability on Protons in the SPS*, CERN Report CERN-AB-2004-055, 2004.

[11] E. Métral, *Stability Criteria for High-Intensity Single-Bunch Beams in Synchrotrons*, CERN Report CERN/PS 2002-022 (AE), 2002.